JURNAL geografi

https://jurnal.unimed.ac.id/2012/index.php/geo/article/view/36866
https://doi.org/10.24114/jg.v15i2.36866 - (Vol 15, No 2 - 2023)
available at http://jurnal.unimed.ac.id/2012/index.php/geo
e-issn (2549-7057) & p-issn (2085-8167)

Monitoring Aerosol Optical Depth for Air Quality Through Himawari-8 in Urban Area West Java Province Indonesia

Riki Ridwana[1,2*], Shafira Himayah[1], Muh Fiqri Abdi Rabbi[1], Izma Maulana Ahmad Lugina[1], Azhari Al Kautsar[1], Anjar Dimara Sakti[3]

[1]Geography Information Science Study Program, Faculty of Social Sciences Education, Universitas Pendidikan Indonesia, Jawa Barat, Indonesia.

[2]Doctoral Program in Geography, Faculty of Geography, Universitas Gadjah Mada, Yogyakarta, Indonesia

[3]Remote Sensing and Geographic Information Science Research Group, Faculty of Earth Sciences and Technology, Institut Teknologi Bandung, Jawa Barat, Indonesia

ARTICLE INFO

Article History:
Received: July 17, 2022
Revision: August 17, 2023
Accepted: August 17, 2023

Keywords:
Aerosol Optical Depth (AOD)
Air Quality
Himawari-8

Corresponding Author
E-mail: rikiridwana@upi.edu

ABSTRACT

Air quality is a crucial parameter in human life. One air quality indicator can be observed through Aerosol Optical Depth (AOD). If these substances are pollutants such as particulate matter, aerosols, and ozone, it is confident that air quality will deteriorate, threatening human health and causing climate change. AOD monitoring can be used as a basis for policymakers and related parties to maintain the stability of air quality in the atmosphere. Many ground observation stations monitor air quality by obtaining data on PM2.5 and PM10 aerosol particles. However, the number of ground stations is limited, resulting in incomplete data. Fortunately, remote sensing satellites have the advantage of covering large areas and providing continuous observations, with the ability to gather information on large-scale aerosol and obtain spatiotemporal distribution. Therefore, this research aims to obtain AOD through Himawari-8 and analyze the spatiotemporal air quality in urban areas of West Java based on AOD. The research methodology used in this study is descriptive analysis with an empirical research approach. Assisted by remote sensing technology and Geographic Information Systems, this research generates AOD data extraction that can be obtained from the new generation satellite of Himawari-8. The distribution of AOD levels and spatiotemporal monitoring in urban areas of West Java is very dynamic depending on anthropogenic activity in a particular area and time.

INTRODUCTION

The rapid urban development and industrial acceleration in recent decades have exacerbated air pollution issues (Gao et al., 2017). High levels of aerosol particles degrade air quality in human living environments (Monks et al., 2009), and they also have implications for climate and human health (Anderson et al., 2012), increasing the risk of cardiovascular diseases, respiratory illnesses and lung cancer (Dominici et al., 2006). Therefore, it is crucial to accurately investigate the properties of aerosols originating from various sources (Wang et al., 2020). Many ground observation stations, such as air quality monitoring stations, have been established to monitor air quality by obtaining data on PM2.5 and PM10 aerosol particles (Hao & Xie, 2018; Zhang et al., 2019).

However, it is challenging to fully understand the large-scale distribution, sources, and movement of aerosol pollution. This limitation arises from the limited number of ground stations, resulting in incomplete data (Morawska et al., 2018). Remote sensing satellites have the advantage of covering vast areas and providing continuous observations, with the ability to collect information on large-scale aerosols and obtain spatiotemporal distributions (Lin et al., 2015; Sakti et al., 2023; Ridwana et al., 2020). Therefore, remote sensing satellites help monitor particulate matter aerosol pollution.

Remote sensing satellites provide a cost-effective means of monitoring aerosol optical depth (AOD), representing the integrated coefficient of aerosol column concentrations and their impact on solar radiation (Holben et al., 1998). Several related studies have concluded that satellite data can be used to analyze the distribution and variation of AOD on a large spatial scale (Levy et al., 2010) and monitor the occurrence of thick haze events (Che et al., 2014). Since the early 20th century, AOD monitoring based on polar-orbiting satellite data has proven viable. Various algorithms have been developed for monitoring AOD values, including single-channel algorithms based on Advanced Very High-Resolution Radiometer (AVHRR) data (Ignatov & Stowe, 2002), multi-angle algorithms based on Multi-angle Imaging SpectroRadiometer (MISR) data, and algorithms based on Dark Target (DT) and Deep Blue (DB) approaches using MODIS data (Hsu et al., 2004).

Compared to polar-orbiting satellites with high spatial resolution but limited temporal resolution, geostationary satellites have the advantage of much higher temporal resolution. These satellites can provide continuous daytime observations of AOD on a large spatial scale. Several AOD retrieval algorithms have been developed based on data from different geostationary satellites. For example, Knapp (2002) studied AOD monitoring in South America using visible channel observations from the Geostationary Operational Environmental Satellite (GOES). Studies in the eastern United States, such as (Knapp et al., 2005), utilized visible imagery from GOES-8 over the past 28 days and selected the darkest pixels to estimate surface reflectance and retrieve AOD observations. This improved method demonstrated that AOD observations under unbiased conditions varied seasonally. Prados et al. (2007) evaluated the GOES Aerosol/Smoke Product (GASP) AOD from GOES-12 compared with AOD from AERONET and MODIS products in North America. Statistical analysis indicated that the GASP/AERONET mean correlation reached 0.79 with a low root mean square difference of 0.13. The GASP/MODIS correlation exceeded 0.7 under increased AOD in the summer of 2004 (Wang, 2003) developed a visible single-channel algorithm with a dynamic aerosol model to retrieve AOD over the western Pacific Ocean based on hourly geostationary Meteorological Satellite (GMS-5) imagery. The retrieval from GMS-5 was consistent with aircraft measurements and AERONET (Wang et al., 2003). (Kim et al., 2008) determined that single-channel AOD algorithms had limitations in retrieving AOD and proposed a new multi-channel AOD algorithm based on mid-infrared and visible channel data from the Multi-functional Transport Satellite (MTSAT-1R).

Himawari-8 is a geostationary meteorological satellite launched in October 2014. It carries the Advanced Himawari Imager (AHI), which utilizes three visible channels and 13 infrared channels with a spatial resolution of 0.5–2 km and a temporal resolution of 10 minutes (Bessho et al., 2016). The AOD retrieval algorithm is based on the surface model of the AHI in the visible channels. This surface model is based on the lowest reflectance corrected for gas with residual aerosol over urban areas or the minimum reflectance calculated using the modified Kaufman method. However, AHI version 1.0 and 2.0 aerosol products have shown large-scale uncertainties (Zhang et al., 2018). Gupta et al. (2019) conducted a study indicating that AHI has six bands similar to MODIS for AOD retrieval and applied the Dark Target (DT) AOD algorithm using AHI observations during the Korea-United States Air Quality

(KORUS-AQ) campaign. This new AHI AOD product agreed well with East Asia's AERONET and MODIS AOD products.

Despite the availability of AOD retrieval from satellite observations using the Dark Target (DT) and Deep Blue (DB) methods, there are still several limitations: (1) Satellite remote sensing of aerosols mainly relies on single algorithms, and the comprehensive utilization of various algorithms is relatively rare. (2) Currently, the spatial resolution of AOD products is generally low. For example, the latest version C6.1 of MODIS aerosol products, including MOD/MYD04_3K (DT) and MOD/MYD04_L2 (DT, DB, and Merged DT-DB), has spatial resolutions of 3 km and 10 km, respectively (Ali & Assiri, 2019).

In urban areas with complex surface characteristics, such as West Java Province, Indonesia, low spatial resolution AOD is insufficient for monitoring air pollution and environmental assessment needs. Therefore, aerosol products with higher spatial resolution than the previous series of satellite image data are required to analyze particulate matter's pollution sources and transmission to understand urban air pollution issues better. Based on the background and problem formulation mentioned above, this research aims to monitor the spatiotemporal air quality in urban areas of West Java using the (AOD) parameter derived from Himawari-8 satellite data.

RESEARCH METHODS

The study area of this research consists of urban areas in the province of West Java, Indonesia (Figure 1). Including the city of Bandung as the provincial capital, the city of Bekasi and its surrounding areas, the district of Karawang and its surrounding areas, the city of Bogor and its surrounding areas, the city of Sukabumi and its surrounding areas, the city of Tasikmalaya and its surrounding areas, the city of Cirebon and its surrounding areas, and other rapidly developing cities in terms of economy and industry (Figure 1). Remote sensing technology and Geographic Information Systems (GIS) are utilized in the research. Himawari-8 remote sensing is used for data processing to obtain AOD, while the GIS is used for analyzing the spatiotemporal air quality levels in urban areas.

This study utilized various materials and tools to obtain primary and secondary data. These include the 1:25,000 scale Rupa Bumi Indonesia (RBI) Map, obtained from the ina-geoportal website https://tanahair.indonesia.go.id/portal-web, and Himawari-8 satellite imagery obtained from the website https://www.eorc.jaxa.jp/ptree/index.html. The Himawari-8 data recognized are January 17, 19, 22, and 25, 2021.

The population used for the research was the urban areas within West Java Province. The sample is limited to areas with a high population activity, one characterized by more industrial activity than other West Java cities and districts. Samples were selected to represent the population, allowing for observing phenomena or events. The selection of sample areas was based on urban regions experiencing rapid development in the economic and industrial sectors.

Data collection in this study employed a blended research concept, which combined digital elements utilizing software and virtual components utilizing internet networks as a communication system. The obtained data were primarily quantitative and were analyzed using the Sataid GMSLPD software with the AOD method to measure the concentration of aerosol presence in the air. The resulting data will serve as a reference indicator for determining the air quality in the urban areas of West Java Province.

To perform AOD extraction from satellite images, several steps and algorithms were followed based on (Wang et al., 2020), using the radiation transmission algorithm for retrieving aerosols over land.

$$\rho TOA(\mu S, \mu 7, \phi) = \rho 0(\mu S, \mu 7, \phi) + T(\mu s)T(\mu v)\rho s(\mu s,\mu v,\phi)/[1- \rho s(\mu s,\mu v,\phi)S] \quad (1)$$

Where:
ρo = Atmosphere path reflectance
T = Atmospheric transmittance function
S = Atmospheric backscatter ratio
ρs = Angular spectral surface reflectance
ρTOA(μS,μ7,ϕ) = The values of solar zenith angle, satellite zenith angle, and relative azimuth angle for each channel.

After obtaining the radiation transmission values, the next step is to calculate the TOA estimation in the blue channel (μm = 0.46) using the equation $\rho TOA\_0.46\ est$ (2). Subsequently, the bias function is calculated using the equation $|\rho TOA\_0.46\ estobs - OA0.46$ (3).

The minimum bias value is selected, and linear interpolation is performed to obtain the AOD values. The obtained AOD values are then validated through field measurements. The Himawari-8 satellite, with a temporal resolution of 10 minutes, is well-suited for conducting temporal analysis. If the algorithm successfully retrieves AOD values at one time, the data can be further processed for different periods.

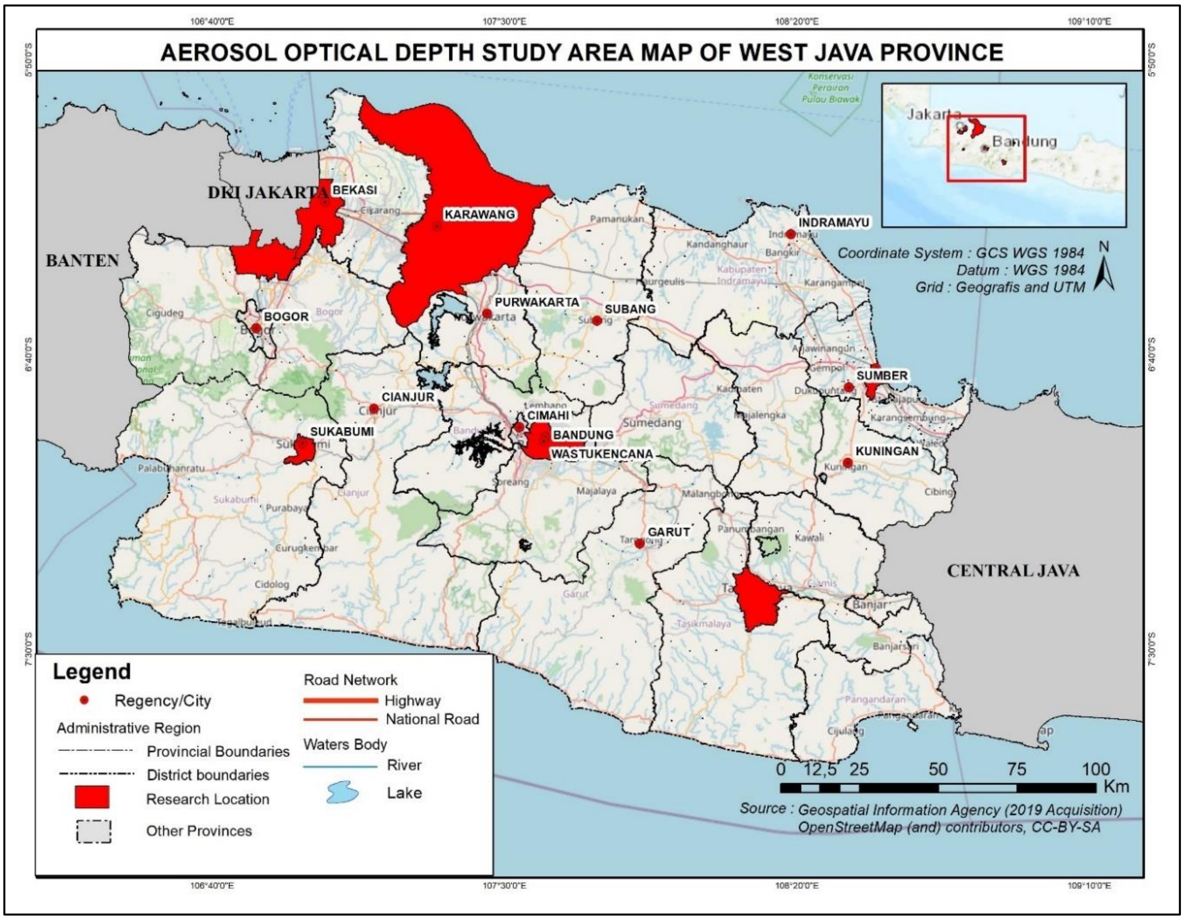

Figure 1. Study area location in West Java Province, Indonesia
(Source: Data Processing, 2021)

RESULT AND DISCUSSION

Data Acquisition of Himawari-8 Images

In this study, the acquired Himawari-8 image data includes the AOD L2 data with a temporal resolution of 10 minutes and the AOD L3 data with a temporal resolution of 1 hour, both having a spatial resolution of 5 km. The Himawari AOD L2 and L3 products used in this study were recorded from January to June 2021 and downloaded from the website http://www.eorc.jaxa.jp/ptree/index.html. On the JAXA website, the AOD data was obtained from the Aerosol Property (ARP) Product of Himawari-8. The ARP Himawari-

8 data was then downloaded from the respective directories based on the specified dates and times. The Himawari-8 image downloading process was divided into six temporal data sets from January to June. The data acquisition was performed at specific times, which remained the same for each period. This was done to observe the movement and changes in AOD values in the study area over time. In this study, the data acquisition was carried out from 06:00 to 07:30 in the morning and from 11:00 to 12:30 in the afternoon. The different data acquisition timing was implemented to examine the relationship between AOD values under different temperature and solar radiation intensity conditions in the same area. This is because AOD values are strongly influenced by temperature, and solar irradiance significantly affects the AOD concentration in the atmosphere.

Processing of Himawari-8 Image Data

The downloaded Himawari AOD data from the Aerosol Property (ARP) Product was visualized using the GrADS software (Figure 2). In this stage, the Himawari-8 image data was input into the GrADS software to display landscape visualization. From the processing, four types of data were obtained. AOD L2 and L3, as well as Aerosol Optical Thickness (AOT) L2 and L3. Figure 3 illustrates the visualization of the Himawari-8 image data in GrADS. To proceed with the data extraction stage, the Himawari-8 image data in netCDF format was converted to TIFF format to facilitate further processing. The data format conversion was performed using Python programming, specifically the GDAL library, to process netCDF data. Alternatively, the conversion can be done directly using the Make NetCDF Raster Layer tool. Figure 4 shows the visualization of the AOD data in TIFF format.

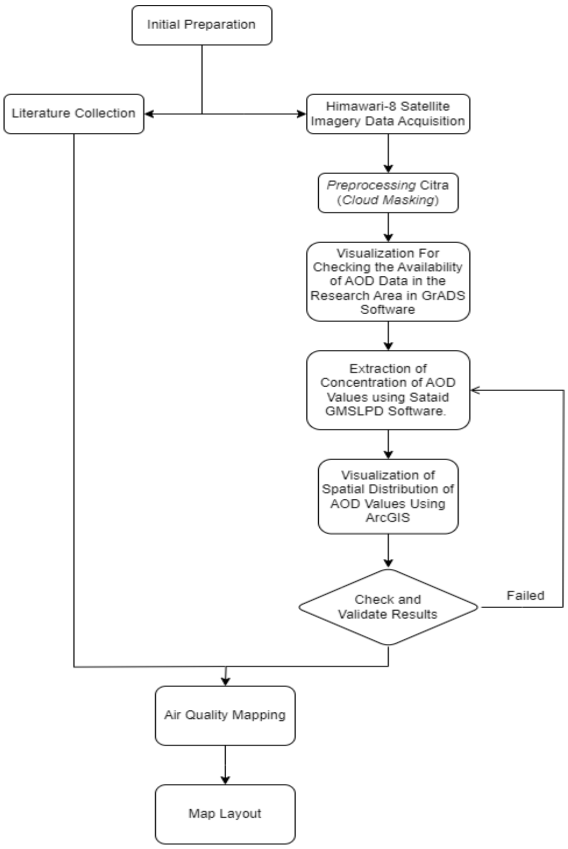

Figure 2. Processing of Himawari-8 Image Data (Source: Data Processing, 2021).

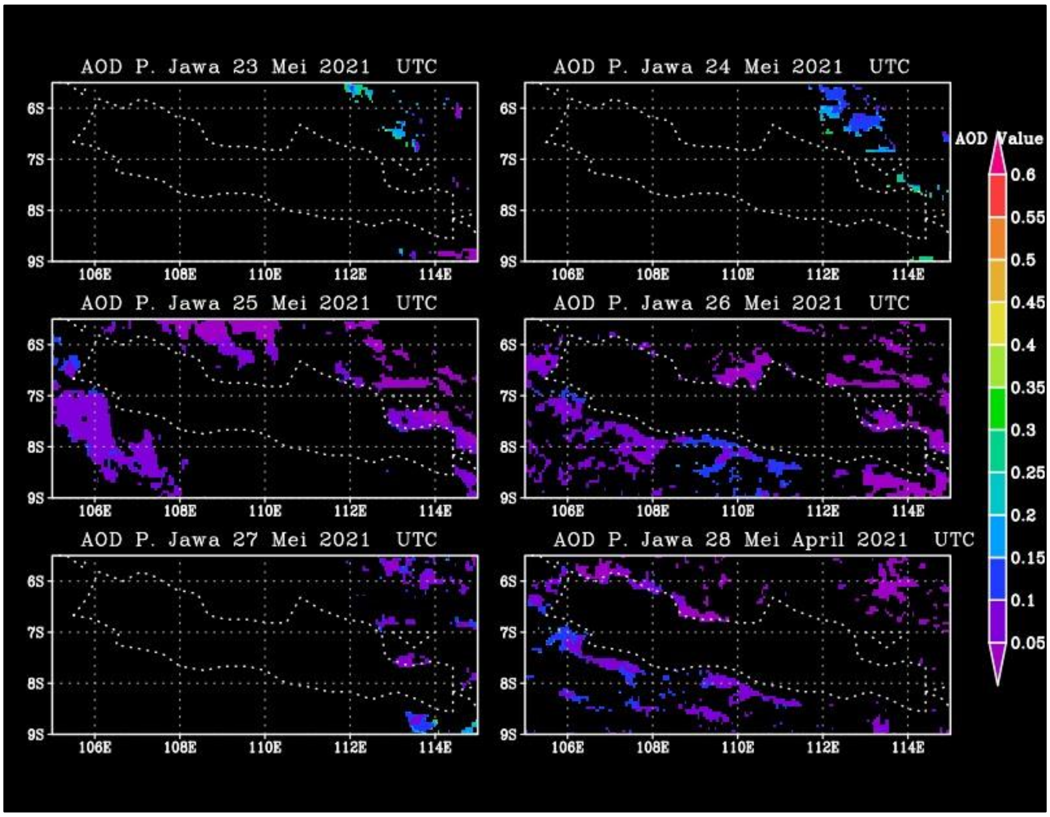

Figure 3. Visualization of Himawari-8 satellite image data using GrADS (Source: Data Processing, 2021)

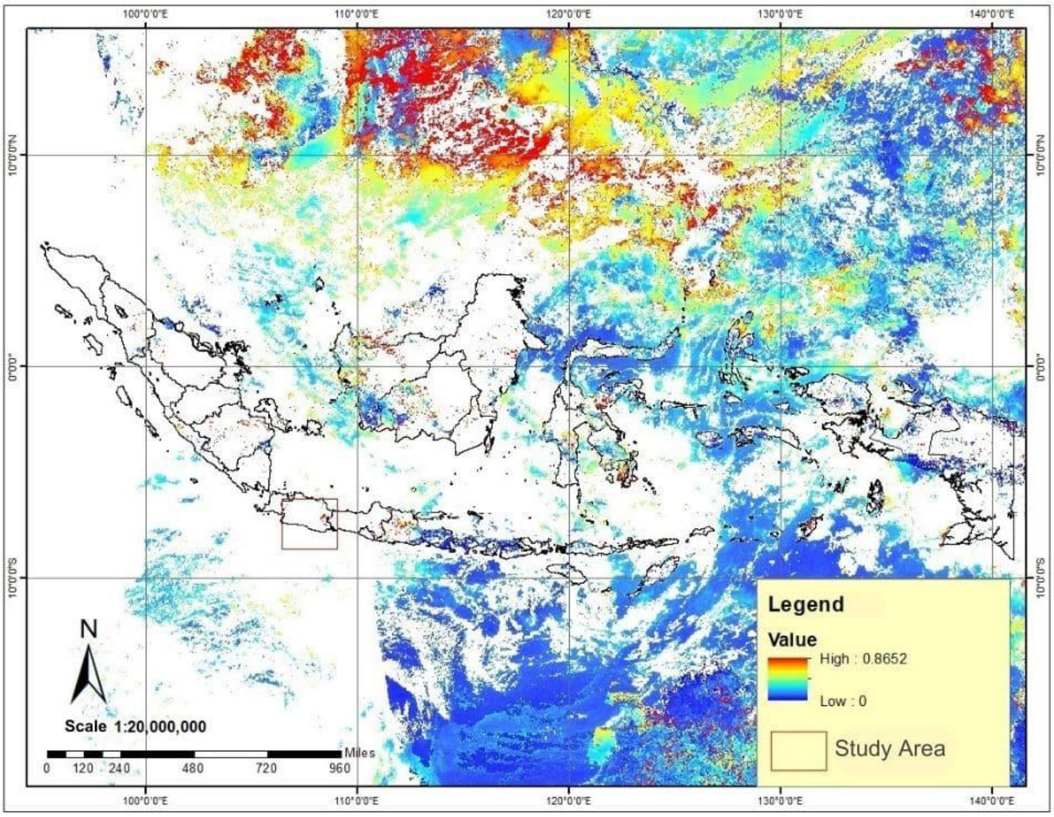

Figure 4. AOD data visualization in tif format (Source: Data Processing, 2021)

Ektraksi Aerosol Optical Depth (AOD)

The AOD data extraction is performed using TIFF-formatted data. The AOD data in TIFF format is extracted using the "Extract Multi Values to Point" tool. Before that, sample points are created according to the study area with available Himawari-8 AOD data. The extraction is carried out for all specified sample dates. The extracted data is then classified based on the date of data recording, location, file name, and values, which consist of AOD and AOT values. The following is an example tabulation of the extracted AOD data classified in Table 1.

Table 1. Classification of Extracted AOD Data

No.	Acquisition date	AOD value	AOT value
1.	17 January 2021	0.4403703511	0.2809963226
		0.4376388788	0.2828500271
		0.4333333075	0.3404648006
2.	19 January 2021	0.5699999929	0.3137999773
3.	22 January 2021	0.5167360902	0.3642503917
		0.4956481457	0.5892593265
		0.5488426089	0.573925972
		0.4105092585	0.8353480697
		0.5009259582	0.5119012594
		0.3432407677	0.9283661246
		0.3973147869	0.6727852225
		0.4241666496	0.6803999543
		0.5255092382	0.4308148921
4.	25 January 2021	0.7084721923	0.02424449287
		0.6015277505	0.9233555794

(Source: Data Processing, 2021).

Monitoring AOD for Air Quality Control in Urban Areas of West Java

The spatial distribution of the monthly average AOD L2 in West Java Province for April at 07:00 AM WIB is shown in Figure 4. During April at 07:00 AM, the Himawari-8 AOD L2 product indicates higher AOD concentrations in Bandung City, Karawang, Cirebon City, and Depok City, densely populated and industrialized regions. The red represents these areas, indicating a concentration value of 2. This means that as the AOD concentration value approaches 2, the AOD concentration becomes higher. Conversely, when the value approaches 1, it indicates a lower AOD concentration, as shown in Figure 4. Based on the data visualization, most areas in West Java have relatively low concentration levels, indicated by the blue colour. However, the larger cities in the region have high AOD levels.

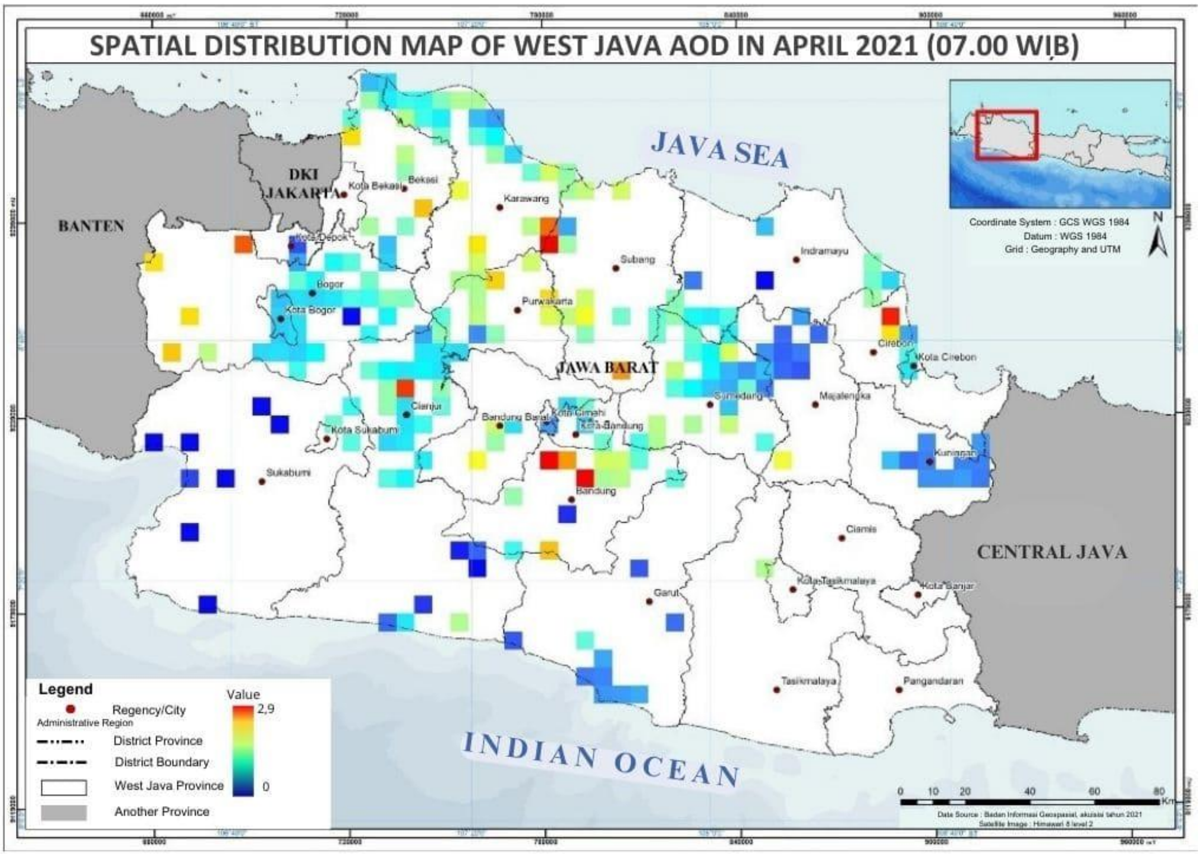

Figure 5. Spatial distribution map of AOD in West Java in April 2021 at 07:00 AM WIB (Source: Data Processing, 2021)

During April at 12:00 PM WIB, the Himawari-8 AOD L2 product indicates higher AOD concentrations in the southwestern region of West Java, including Sukabumi and Cianjur. The distribution of AOD concentrations in the West Java region in April at 12:00 PM shows that densely populated urban areas have low AOD values, except for some points in Cimahi City, Depok City, Bekasi Regency, and Karawang. These areas are represented by red-yellow colours, indicating concentrations approaching 1.4. This means that as the AOD concentration value approaches 1.4, the AOD concentration becomes higher, while values approaching 0 indicate low AOD concentration, as seen in Figure 6.

During May at 07:00 AM WIB, the Himawari-8 AOD L2 product indicates higher AOD concentrations in the eastern and northern regions of West Java, including Ciamis, Pangandaran, Subang, and Indramayu. These areas are densely populated and industrialized. The areas are represented by red, indicating concentrations of 2. This means that as the AOD concentration value approaches 2, the AOD concentration becomes higher, while values approaching 1 indicate low AOD concentration, as shown in Figure 7.

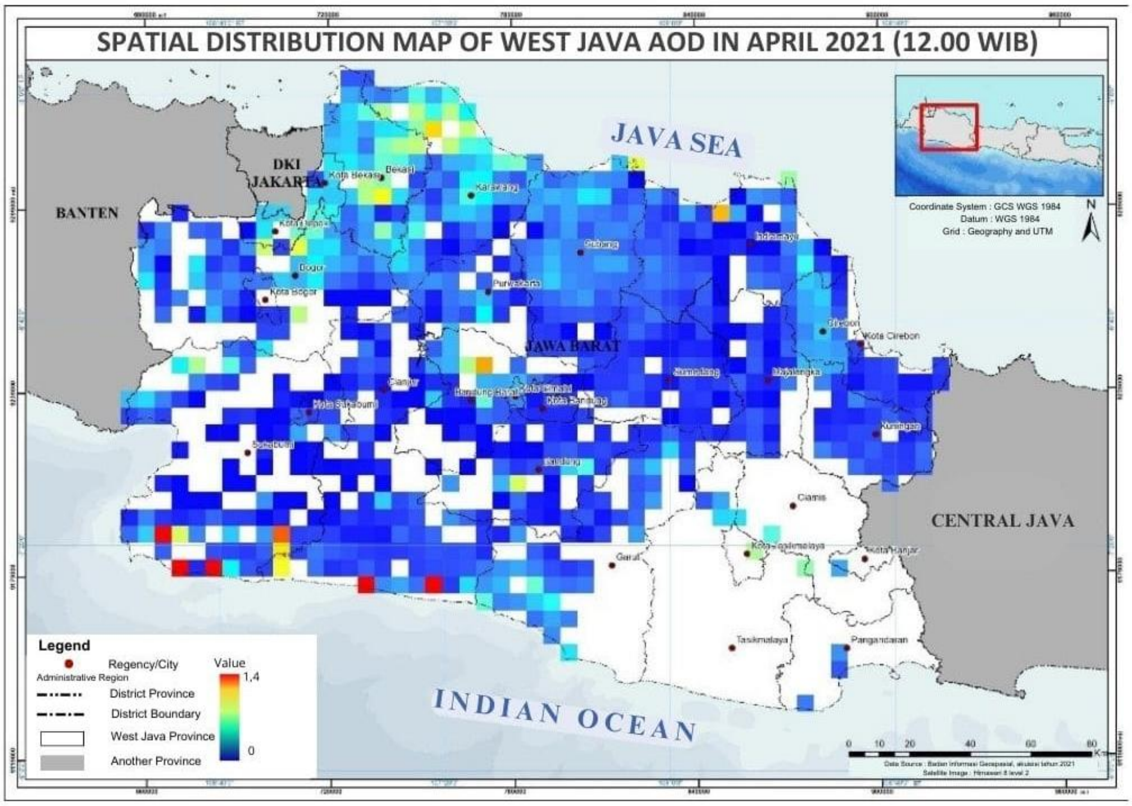

Figure 6. Spatial distribution map of AOD in West Java in April 2021 at 12:00 PM WIB (Source: Data Processing, 2021)

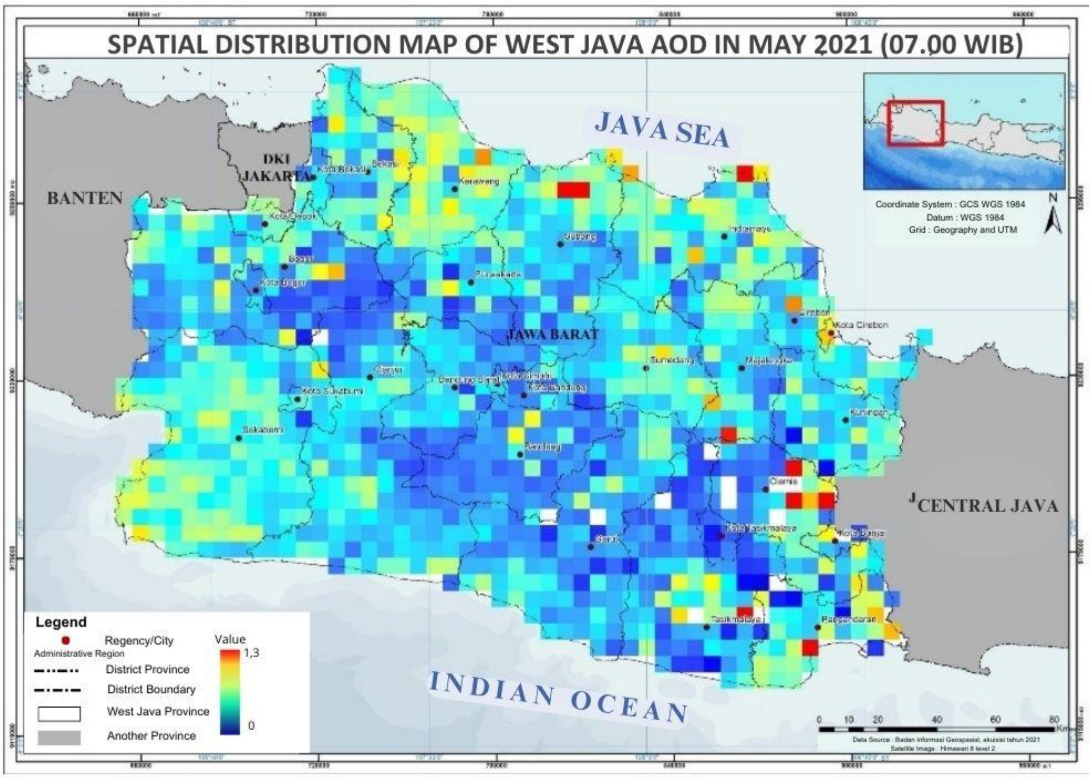

Figure 7. Spatial distribution map of AOD in West Java in May 2021 at 07:00 AM WIB (Source: Data Processing, 2021)

During May at 12:00 PM WIB, the Himawari-8 AOD L2 product indicates higher AOD concentrations in the eastern region of West Java, particularly in the southeastern and central parts, including Ciamis, Pangandaran, Majalengka, Sumedang, Bandung City, and the surrounding areas. High AOD values are also identified in the eastern part of Depok City. This distribution differs from the AOD distribution at 07:00 AM in May. These areas are represented by red, indicating concentrations with a value of 2.2. This means that as the AOD concentration value approaches 2.2, the AOD concentration becomes higher, while values approaching 1 indicate low AOD concentration. The AOD values in urban areas of West Java exhibit significant spatial and temporal dynamics, influenced by variations in time and anthropogenic activities such as industrial and transportation activities. At 07:00 AM and 12:00 PM local time, peak activity times for the population, diverse AOD distributions are observed in each urban area of West Java, which can be monitored using Himawari-8 imagery. Similar phenomena have also been observed in neighbouring countries, such as Malaysia, as previously studied (Zaman & Kanniah, 2020).

Anthropogenic activity affecting AOD concentrations has also been proven by research (Kanniah et al., 2020), which can be seen from the decrease in AOD values due to the lockdown due to COVID-19 on spatiotemporal variations of atmospheric pollutants in Southeast Asia, particularly in Malaysia, Singapore, Brunei Darussalam, and the Philippines.

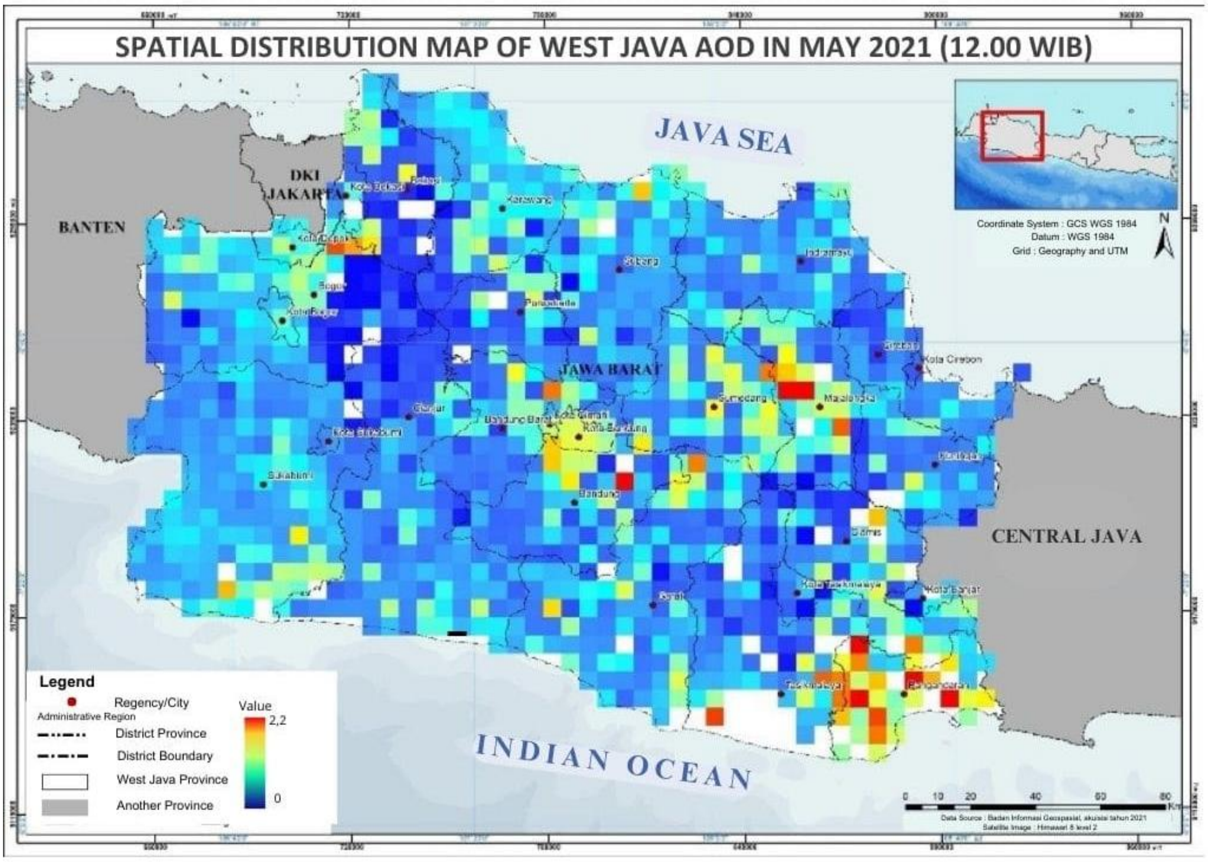

Figure 8. Spatial distribution map of AOD in West Java in May 2021 at 12:00 PM WIB
(Source: Data Processing, 2021)

CONCLUSION

Air quality monitoring stations, limited in availability in Indonesia, can be monitored using multitemporal monitoring via remote sensing satellite imagery. We have proven case studies related to this matter to identify air quality in West Java urban areas effectively and efficiently using Himawari-8 imagery. The data allows visualization of the spatial distribution of AOD based on monthly and hourly averages. Based on our analysis, the spatial distribution and pattern of AOD in urban areas of West Java are very dynamic, with concentration levels varying from time to time depending on the level of air pollution, especially from industrial and transportation activities and other anthropogenic activities.

ACKNOWLEDGMENT

The author would like to thank the Geography Information Science Study Program, Faculty of Social Sciences Education, Universitas Pendidikan Indonesia for funding this research. Additionally, the author would like to thank JAXA for providing access to AOD data through their Aerosol Property (ARP) Product Himawari-8 website.

REFERENCES:

Ali, M. A., & Assiri, M. (2019). Analysis of AOD from MODIS-Merged DT–DB Products Over the Arabian Peninsula. Earth Systems and Environment, 3(3), 625–636. https://doi.org/10.1007/s41748-019-00108-x.

Anderson, J. O., Thundiyil, J. G., & Stolbach, A. (2012). Clearing the Air: A Review of the Effects of Particulate Matter Air Pollution on Human Health. Journal of Medical Toxicology, 8(2), 166–175. https://doi.org/10.1007/s13181-011-0203-1.

Bessho, K., Date, K., Hayashi, M., Ikeda, A., Imai, T., Inoue, H., Kumagai, Y., Miyakawa, T., Murata, H., Ohno, T., Okuyama, A., Oyama, R., Sasaki, Y., Shimazu, Y., Shimoji, K., Sumida, Y., Suzuki, M., Taniguchi, H., Tsuchiyama, H., … Yoshida, R. (2016). An introduction to Himawari-8/9 — Japan's new-generation geostationary meteorological satellites. Journal of the Meteorological Society of Japan, 94(2), 151–183. https://doi.org/10.2151/jmsj.2016-009

Che, H., Xia, X., Zhu, J., Li, Z., Dubovik, O., Holben, B., Goloub, P., Chen, H., Estelles, V., Cuevas-Agulló, E., Blarel, L., Wang, H., Zhao, H., Zhang, X., Wang, Y., Sun, J., Tao, R., Zhang, X., & Shi, G. (2014). Column aerosol optical properties and aerosol radiative forcing during a serious haze-fog month over North China Plain in 2013 based on ground-based sunphotometer measurements. Atmospheric Chemistry and Physics, 14(4), 2125–2138. https://doi.org/10.5194/acp-14-2125-2014

Dominici, F., Peng, R. D., Bell, M. L., Pham, L., McDermott, A., Zeger, S. L., & Samet, J. M. (2006). Fine particulate air pollution and hospital admission for cardiovascular and respiratory diseases. Journal of the American Medical Association, 295(10), 1127–1134. https://doi.org/10.1001/jama.295.10.1127.

Gao, J., Woodward, A., Vardoulakis, S., Kovats, S., Wilkinson, P., Li, L., Xu, L., Li, J., Yang, J., Li, J., Cao, L., Liu, X., Wu, H., & Liu, Q. (2017). Haze, public health and mitigation measures in China: A review of the current evidence for a further policy response. Science of the Total Environment, 578, 148–157. https://doi.org/10.1016/j.scitotenv.2016.10.231.

Gupta, P., Levy, R. C., Mattoo, S., Remer, L. A., Holz, R. E., & Heidinger, A. K. (2019). Applying the Dark Target aerosol algorithm with Advanced Himawari Imager observations during the KORUS-AQ field campaign. Atmospheric Measurement Techniques, 12(12), 6557–6577. https://doi.org/10.5194/amt-12-6557-2019.

Hao, Y., & Xie, S. (2018). Optimal redistribution of an urban air quality monitoring network using atmospheric dispersion model and genetic algorithm. Atmospheric Environment, 177, 222–233. https://doi.org/10.1016/j.atmosenv.2018.01.011.

Holben, B. N., Eck, T. F., Slutsker, I., Tanré, D., Buis, J. P., Setzer, A., Vermote, E., Reagan, J. A., Kaufman, Y. J., Nakajima, T., Lavenu, F., Jankowiak, I., & Smirnov, A. (1998). AERONET - A federated instrument network and data archive for aerosol characterization. Remote Sensing of Environment, 66(1), 1–16. https://doi.org/10.1016/S0034-4257(98)00031-5.

Hsu, N. C., Tsay, S. C., King, M. D., & Herman, J. R. (2004). Aerosol properties over bright-reflecting source regions. IEEE Transactions on Geoscience and Remote Sensing, 42(3), 557–569. https://doi.org/10.1109/TGRS.2004.824067.

Ignatov, A., & Stowe, L. (2002). Aerosol retrievals from individual AVHRR channels. Part I: Retrieval algorithm and transition from Dave to 6S radiative transfer model. Journal of the Atmospheric Sciences, 59(3 PT 1), 313–334. https://doi.org/10.1175/1520-0469(2002)059<0313:arfiac>2.0.co;2.

Kamarul Zaman, N. A. F., & Kanniah, K. D. (2020). Spatio-temporal assessment of Aerosol Optical Depth from Himawari-8 satellite data over Malaysia. IOP Conference Series: Earth and Environmental Science, 540(1). https://doi.org/10.1088/1755-1315/540/1/012053.

Kanniah, K. D., Zaman, N. A. F. K., Kaskaoutis, D. G., & Latif, M. T. (2020). COVID-19's impact on the atmospheric environment in the Southeast Asia region. Science of the Total Environment, 736, 139658.

Kim, J., Yoon, J. M., Ahn, M. H., Sohn, B. J., & Lim, H. S. (2008). Retrieving aerosol optical depth using visible and mid-IR channels from geostationary satellite MTSAT-1R. International Journal of Remote Sensing, 29(21), 6181–6192. https://doi.org/10.1080/01431160802175553.

Knapp, Ken R., Frouin, R., Kondraguntas, S., & Prados, A. (2005). Toward aerosol optical depth retrievals over land from GOES visible radiances: Determining surface reflectance. International Journal of Remote Sensing, 26(18), 4097–4116. https://doi.org/10.1080/01431160500099329.

Knapp, Kenneth R., Vonder Haar, T. H., & Kaufman, Y. J. (2002). Aerosol optical depth retrieval from GOES-8: Uncertainty study and retrieval validation over South America. Journal of Geophysical Research: Atmospheres, 107(7–8). https://doi.org/10.1029/2001jd000505.

Levy, R. C., Remer, L. A., Kleidman, R. G., Mattoo, S., Ichoku, C., Kahn, R., & Eck, T. F. (2010). Global evaluation of the Collection 5 MODIS dark-target aerosol products over land. Atmospheric Chemistry and Physics, 10(21), 10399–10420. https://doi.org/10.5194/acp-10-10399-2010.

Lin, C., Li, Y., Yuan, Z., Lau, A. K. H., Li, C., & Fung, J. C. H. (2015). Using satellite remote sensing data to estimate the high-resolution distribution of ground-level PM2.5. Remote Sensing of Environment, 156, 117–128. https://doi.org/10.1016/j.rse.2014.09.015.

Monks, P. S., Granier, C., Fuzzi, S., Stohl, A., Williams, M. L., Akimoto, H., Amann, M., Baklanov, A., Baltensperger, U., Bey, I., Blake, N., Blake, R. S., Carslaw, K., Cooper, O. R., Dentener, F., Fowler, D., Fragkou, E., Frost, G. J., Generoso, S., … von Glasow, R. (2009). Atmospheric composition change - global and regional air quality. Atmospheric Environment, 43(33), 5268–5350. https://doi.org/10.1016/j.atmosenv.2

009.08.021.

Morawska, L., Thai, P. K., Liu, X., Asumadu-Sakyi, A., Ayoko, G., Bartonova, A., Bedini, A., Chai, F., Christensen, B., Dunbabin, M., Gao, J., Hagler, G. S. W., Jayaratne, R., Kumar, P., Lau, A. K. H., Louie, P. K. K., Mazaheri, M., Ning, Z., Motta, N., … Williams, R. (2018). Applications of low-cost sensing technologies for air quality monitoring and exposure assessment: How far have they gone? Environment International, 116(February), 286–299. https://doi.org/10.1016/j.envint.2018.04.018.

Prados, A. I., Kondragunta, S., Ciren, P., & Knapp, K. R. (2007). GOES Aerosol/Smoke Product (GASP) over North America: Comparisons to AERONET and MODIS observations. Journal of Geophysical Research-Atmospheres, 112(15), 1–15. https://doi.org/10.1029/2006JD007968.

Ridwana, R., & Himayah, S. (2020). Utilization of remote sensing technology and geographic information systems for tourism development. International Journal of Applied Sciences in Tourism and Events, 4(2), 158-169. http://dx.doi.org/10.31940/ijaste.v4i2.2042

Sakti, A. D., Anggraini, T. S., Ihsan, K. T. N., Misra, P., Trang, N. T. Q., Pradhan, B., ... & Wikantika, K. (2023). Multi-air pollution risk assessment in Southeast Asia using integrated remote sensing and socio-economic data products. Science of The Total Environment, https://doi.org/10.1016/j.scitotenv.2022.158825.

Wang, J., Christopher, S. A., Brechtel, F., Kim, J., Schmid, B., Redemann, J., Russell, P. B., Quinn, P., & Holben, B. N. (2003). Geostationary satellite retrievals of aerosol optical thickness during ACE-Asia. Journal of Geophysical Research: Atmospheres, 108(23). https://doi.org/10.1029/2003jd003580.

Wang, L., Yu, C., Cai, K., Zheng, F., & Li, S. (2020). Retrieval of Aerosol Optical Depth from the Himawari-8 Advanced Himawari Imager data : Application over Beijing in the summer of 2016. Atmospheric Environment, 241(August), 117788. https://doi.org/10.1016/j.atmosenv.2020.117788.

Zhang, T., Zang, L., Wan, Y., Wang, W., & Zhang, Y. (2019). Ground-level PM2.5 estimation over urban agglomerations in China with high spatiotemporal resolution based on Himawari-8. Science of the Total Environment, 676, 535–544. https://doi.org/10.1016/j.scitotenv.2019.04.299.

Zhang, W., Xu, H., & Zheng, F. (2018). Aerosol optical depth retrieval over East Asia using Himawari-8/AHI data. Remote Sensing, 10(1). https://doi.org/10.3390/rs10010137.